

Supplemental Materials: DeltaPsi.py Version 1.0

DeltaPsi.py is a program for first-order, exploratory simulations of the effects of capacitance, proton buffering capacity and counter-ion movements on the thylakoid proton motive force (pmf), transthylakoid electric field ($\Delta\psi$), stroma-lumen pH difference (ΔpH), linear electron flow (LEF), the ratio of ATP/NADPH produced by LEF, the activation and recovery of the lumen pH-dependent form of nontphotochemical quenching (NPQ), termed q_E , photosystem II (PSII) activity and recombination rates and 1O_2 production.

The code is based on the simulations in [\(Cruz et al. 2001\)](#) because simulations using this code were validated by the review process in both the original publication and in a separate, follow up publications [\(Zaks et al. 2012\)](#). The following describes changes in this version.

- 1) The code was updated to run on modern, open-source, cross-platform and freely-available Python platform. Examples below were performed using the open source Jupyter notebook platform (www.jupyter.org), but code can also be run on any Python platform.
- 2) To provide the maximal transparency and allow others to repeat and modify our code and simulations, the full code is made available on GitHub (www.github.com) with extensive annotation. Readers are encouraged to fork the code and add their modifications, improvements and tests. It is hoped that these open source tools will provide the capacity to extend or modify and extend and validate the simulations, especially to test new hypotheses.
- 3) A more efficient ODE solver, odeint (scipy.integrate.odeint <https://docs.scipy.org/doc/scipy-0.18.1/reference/generated/scipy.integrate.odeint.html>), was used to increase the speed and accuracy of the simulations.
- 3) Several improvements in the formulae were made to include several recent advances, as outlined in the following.
 - a) Explicit simulation of Q_A and plastoquinone (PQ) redox states were included to simulate PSII quantum yields and to account for the effects of $\Delta\psi$ on PSI recombination reactions.
 - b) The lumen pH-dependence of the xanthophyll cycle and the protonation of PsbS were updated to simulate the pH dependencies reported in Takizawa et al. [\(Takizawa et al. 2007\)](#) and Zaks et al. [\(Zaks et al. 2012\)](#).
 - c) The effects of lumen pH on plastoquinol (PQH_2) oxidation at the cytochrome b_6f complex were included to account for the observed “photosynthetic control” of electron transfer by the lumen pH, using the model and pK_a values reported in [\(Takizawa et al. 2007\)](#).
 - d) The driving force for ATP synthase reaction (and thus the efflux of protons) is now taken as being equal to the difference in the proton motive force (pmf) and the free energy storage in ATP (ΔG_{ATP}) divided by n , the stoichiometry of H^+ translocated through the ATP synthase over the number of molecules of ATP formed, as described in more detail below.
 - e) A more realistic model for the kinetics of the cytochrome b_6f complex were developed, to account for the thermodynamic and kinetic effects of pmf components on these reactions. In particular, the code now considers the b_6f complex to be fully reversible, so that both Dy and DpH alter the equilibrium constant.
 - f) An equation was derived and implemented to calculate the quantum efficiency of PSII based on NPQ and Q_A redox state.

Table S1. Static and slowly-changing parameters. Table 1 describes the static, or slowly changing, parameters used in model; these constants are not updated by the odeint package, but can be updated between sub-sets . Baseline (standard) values and descriptions of the major parameters used in the simulations together with citations are given in Tables 1 and 2, but can be modified at run time, or during the simulations.

Parameter, variable name	Initial Value	Units	Description
standard PSII content, max_PSII	1	$X 2 \cdot 10^{-13}$ moles cm^{-2} , $X 6 \cdot 10^{10}$ complexes cm^{-2}	To simplify the calculations, the contents of photosynthetic complexes are normalized to a certain area of the thylakoid membrane, the standard PSII content, or max_PSII. The initial value is taken from the literature to be $6 \cdot 10^{-10}$ complexes cm^{-2} , see (1, 2)
cytochrome b_6f content, b6f_content	1	complex standard PSII content ⁻¹	b6f_content describes the content of cytochrome b_6f complex relative to the standard PSII content. The content and properties of the cytochrome b_6f complex are critical for maintaining photosynthetic control (3-9). Literature values range from substoichiometric to equal to that of PSII, and may change in response to environmental stresses or developmental regulation (10). Changes in this parameter can be compensated by changes in the rate constants.
PSI content, PSI_content	1	complex standard PSII content ⁻¹	Describes the content of PSI centers relative to the standard PSII content. Changes in this parameter can be compensated by changes in the rate constants. A recent review of the literature (10) concluded that the ratio of PSI to PSII is relatively close to 1:1, but can vary from species to species, and in response to environmental stresses or developmental regulation (10).
ATP synthase content, ATP_synthase_content	1	complex standard PSII content ⁻¹	Describes the content of ATP synthase centers relative to the standard PSII content. Changes in this parameter can be compensated by changes in the rate constants.
lumen volume per standard PSII content lumen_protons_per_turnover	$6.7 \cdot 10^{-21}$	L complex ⁻¹	The lumen volume for each standard PSII content, derived from the estimated lumen volume per area of thylakoid (11). In this version, the volume is held constant, but in reality is expected to change with altered stromal and luminal osmotic potentials, as reviewed in (12).
n, n	4.67	scalar	The stoichiometry of moles of protons translocated through the ATP synthase per mole of ATP produced. The value of n can be estimated based on the mechanistic model for ATP synthase and the observed stoichiometry of the c subunit ring in thylakoids ($c_subunits_per_ATP_synthase = 14$ (13), indicating 14 protons translocated for a complete rotation of the and the number of ATP molecules made for a full rotation of the F_1 subcomplex = 3 (14), suggesting that $n = 4.67$
ΔG_{ATP} , DeltaGatp_KJ_per_mol	40-45 kJ/mol	kJ/mol	ΔG_{ATP} is the free energy stored in stromal ATP/ADP + Pi couple. ΔG_{ATP} is thought to remain relatively constant under steady-state conditions, between 40-45 kJ/mol, but can change under fluctuating light (15).
ΔG_{ATP} (eV) DeltaGatp	0.42-0.47	eV	ΔG_{ATP} , expressed in electron volts.
pH_{stroma} , pHstroma_initial	7.8	pH units	The pH of the stromal compartment. Literature values for pH_{stroma} range from 7.5 to 8, and is thought to be higher during photosynthesis (16, 17). The pH of the stroma (considered to be constant in this version of the simulation).

$V_{\max}(\text{VDE})$, VDE_max_turnover_number	1	$\text{s}^{-1} \text{ PSII}^{-1}$	Because we do not have reliable information on the ratio of VDE to PSII, this value is modulated to roughly match the observed rates of zeaxanthin accumulation.
$\text{pK}_a(\text{VDE})$, pKvde	5.8	pH units	$\text{pK}_a(\text{VDE})$ is the effective pK_a for protonation of the violaxanthin de-epoxidase (VDE), that results in the activation of the enzyme (18).
Hill coefficient for VDE activation, VDE_Hill	4	scalar	Empirical fitting of Z accumulation to in vivo estimates of lumen pH are consistent with a range of values reported for isolated thylakoids (18-20). Modulating this parameter from 1-5 affected results quantitatively, but did not alter the major trends.
rate constant for ZE, kZE	0.01	s^{-1}	The value of kZE was taken from Takizawa et al. (2007), to account for the apparent difference between the pK_a for activation of VDE and the apparent pK_a for accumulation of Z. Note that the zKE reaction is considered to be pseudo-first order with respect to the content of Z, and that any dependence on other substrates (NADPH and O_2) are ignored.
$\text{pK}_a(\text{PsbS})$, pKPsbS	6.0	pH units	$\text{pK}_a(\text{PsbS})$ describes the pK_a for protonation of PsbS, which results in activation of the rapid qE response. The value of kZE was taken from Takizawa et al. (7), based on empirical fits to in vivo estimates.
NPQ_{\max} , max_NPQ	5.8	pH units	NPQ_{\max} is an empirically-derived term describing the relationship between maximum level of NPQ at saturation, when all xanthophyll components are in the Z form, and all PsbS is protonated, so that: $\text{NPQ} = \text{max_NPQ} [\text{PsbS protonation}] [Z]$. The maximum NPQ is known to be dependent on genotype and growth conditions.
$V_{\max}(\text{ATP synthase})$, ATP_synthase_max_turnover	1000	$\text{ATP s}^{-1} \text{ complex}^{-1}$	The maximum turnover rate of ATP synthase.
$C_{\text{thylakoid}}$, Thylakoid_membrane_capacitance	0.6	$\mu\text{F cm}^{-2}$	The thylakoid membrane electrical capacitance (1, 2, 11).
Inverse thylakoid membrane capacitance, Volts_per_charge	0.033	$\text{V charge}^{-1} \text{ standard PSII content}^{-1}$	Volts_per_charge is used to rapidly calculate the membrane voltage generated by charge movements.
P_{K^+} , perm_K	60-6000	$\text{ions s}^{-1} \text{ V}^{-1} \text{ standard PSII content}^{-1}$	P_{K^+} describes the permeability of the thylakoid to K^+ or similar counter-ions. This term is adjusted empirically to modulate the simulated rates of appearance and dissipation of the ΔpH component of pmf . The units are in V^{-1} because as in Cruz et al. 2001, the simulation considers the rate of K^+ movement through the channels to be proportional to pK^+ and the potassium motive force, Kmf , i.e. the sum of the electrical field and concentration differences, calculated as for the pmf , see also below.
$V_{\max}(\text{b}_6\text{f})$, max_b6f	300	$\text{electrons from PQH}_2 \text{ to PC complex}^{-1} \text{ s}^{-1}$	Maximum rate of the cytochrome b_6f complex, when the plastoquinone pool is in the reduced form (PQH_2) and lumen pH is well above the regulatory pK_a . The rate is an average of the individual partial reactions, and a value of about 300 is consistent with the observed rates of photosynthesis and complex stoichiometries.
pK_{reg} , pKreg	6.0	pH units	The pKreg determines pH-dependence of PQH_2 oxidation at the cytochrome b_6f complex. This is a kinetic constraint, likely related to the deprotonation of a His residue on the Rieske FeS protein (21-23). The empirically measured value is between 6.0 and 6.5 (6-9).
$E_{\text{m},7}(\text{PC})$, Em7_PC	0.37	V (versus SHE)	The midpoint potential of plastocyanin at pH=7, expressed as V against standard hydrogen electrode. The midpoint potential of PC is considered to be pH-independent over the physiological range (24).
$E_{\text{m},7}(\text{PQ}/\text{PQH}_2)$, Em7_PQH2	0.11	V (versus SHE)	The midpoint potential of the PQ/ PQH_2 couple at pH=7. This value is pH dependent (22) and is adjusted in the program by -0.06 V per pH unit changes in lumen pH from 7.0.

β_{lumen} , buffering_capacity	0.03	M/pH unit	β_{lumen} describes the dependence of lumen pH on the number of protons introduced. the buffering capacity of the lumen
σ_{PSI} , PSI_antenna_size	1	ratio	σ_{PSI} describes the relative PSI cross section (compared to that of PSII). Setting σ_{PSI} and σ_{PSII} equal will ensure that photosystems receive the same light flux.
$k_{\text{PC} \rightarrow \text{P700}^+}$, k_PC_to_P700	500	$\text{PC}^{-1} \text{ s}^{-1}$	The rate constant for oxidation of PC by P700^+ , with unity concentrations of reduced PC and P700^+ . The reaction is bimolecular, and the rate is determined by the product of $k_{\text{PC} \rightarrow \text{P700}^+}$, the concentration of reduced PC and P700^+ . In version 1.0, the potential complexities of PC interactions with PSI and cytochrome <i>f</i> (25, 26) are simplified in this version of the simulation.
σ_{PSII} , PSII_antenna_size	1	ratio	Describes the relative PSII cross section. See comments on σ_{PSI} .
k_{QA} , kQA	1000	s^{-1}	The rate constant for oxidation of QA^- by PQ. The reaction is simplified as a second-order process between reduced QA^- and oxidized PQ, and thus a rough average of the individual partial reactions (27) that involve a series of electron transfer to Q_B , exchange of PQ and PQH_2 at the Q_B site etc.
k_{recomb} , k_recomb	0.33	s^{-1}	The rate of charge recombination in PSII. The value of k_{recomb} is that for recombination from the S_2QA^- state in the absence of $\Delta\psi$ and ΔpH . The actual value will depend on a number of factors, including the redox state of the oxygen evolving complex, i.e. the S-state as well as $\Delta\psi$ and ΔpH . Some S-states are more or less stable than the S2 state, so the current code assumes the average is close to that from S_2QA^- , which measured in the presence of DCMU but in the absence of an electric field is about 0.3 s ⁻¹ The effects of $\Delta\psi$ and ΔpH are discussed below.
ϕ_{triplets} , triplet_yield	0.45	fraction	The yield of $^3\text{P}_{680}$ triplets arising from PSII recombination events. Recombination produces a high yield of $^3\text{P}_{680}$ ()
$\phi^1_{\text{O}_2}$, triplet to singletO2 yield	1.0	fraction	The yield of $^1\text{O}_2$ from chlorophyll triplets, which is likely to be near unity ().

Table S2. Variable states. Table S2 describes the rapidly changing states of the model, which are updated by the odeint routines. Each of these parameters can change rapidly, and are modified by the odeint solver.

Parameter, variable name	Initial Value	Units	Description
Violaxanthin content, V	1	Relative	The content of violaxanthin in the thylakoid, expressed in relative units.
Zeaxanthin content, Z	1	Relative	The content of zeaxanthin in the thylakoid, expressed in relative units.
PQ, PQ	6	Relative	The number of molecules of plastoquinone (PQ) in its oxidized form, relative to standard PSI content.

PQH ₂ , PQH2	1	Relative	The number of molecules of plastoquinol (PQH ₂) in its oxidized form, relative to standard PSI content.
PC(ox), PC_ox	0	Relative	The number of molecules of plastocyanin (PC) in its oxidized form, relative to standard PSI content.
PC(red), PC_ox	2	Relative	The number of molecules of plastocyanin (PC) in its reduced form, relative to standard PSI content.
<i>pmf</i> , pmf	0.06(ΔpH) + Δψ	V	The total proton motive force, <i>pmf</i> . The initial value is calculated from the sum of energetic contributions from ΔpH and Δψ.
ΔG _{ATP} , DeltaGatp_KJ_per_mol	40-45 kJ/mol	kJ/mol	ΔG _{ATP} is the free energy stored in stromal ATP/ADP + Pi couple. ΔG _{ATP} is thought to remain relatively constant under steady-state conditions, between 40-45 kJ/mol, but can change under fluctuating light (15).
ΔG _{ATP} (eV) DeltaGatp	0.42-0.47	eV	ΔG _{ATP} , expressed in electron volts.
pH _{stroma} , pHstroma	7.8	pH units	The pH of the stromal compartment. Literature values for pH _{stroma} range from 7.5 to 8, and is thought to be higher during photosynthesis (16, 17). The pH of the stroma (considered to be constant in this version of the simulation).
pH _{lumen} , pHlumen	*calculated at run time	pH units	The pH of the lumen.
K ⁺ _{lumen} , Klumen	0.01-0.1	M	The concentration of K ⁺ in the lumen. The current model assumes that all K ⁺ is free, i.e. not bound.
K ⁺ _{stroma} , Kstroma	0.01-0.1	M	The concentration of K ⁺ in the stroma. The current model assumes that all K ⁺ is free, i.e. not bound. In the current model, K ⁺ _{stroma} is assumed to be constant.
Q _A , QA_content	1	relative	The content of oxidized Q _A relative to standard PSII.
Q _A ⁻ , QAm_content	0	relative	The content of semiquinone Q _A ⁻ relative to standard PSII.
P ₇₀₀ ⁺ , P700_ox	0	relative	The content of oxidized P ₇₀₀ ⁺ relative to PSI.
P ₇₀₀ , P700_red	1	relative	The content of reduced P ₇₀₀ relative to PSI.
Fd(ox), Fd_ox	1	relative	The content of oxidized ferredoxin (Fd) relative to standard PSII.
Fd(red), Fd_red	0	relative	The content of reduced ferredoxin (Fd) relative to standard PSII.
NPQ	0	relative	The ratio of rate constant (kNPQ) for regulated nonphotochemical quenching (NPQ) NPQ (kNPQ) relative to the sum of rate constants for non-radiative decay and fluorescence, see text for details.
¹ O ₂ , singletO2	0	relative	The number of ¹ O ₂ molecules produced per standard PSII.

[ATP], <i>ATP_pool</i>	Set by DGATP,	relative	The content of ATP in the stroma relative to standard PSII. The value is set from the initial DGATP value, with ATP+ADP=60
[ADP], <i>ADP_pool</i>	30		The content of ADP in the stroma relative to standard PSII.

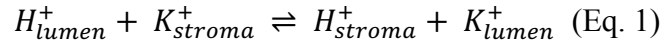
Description of updated code.

The following describes the equations used in the simulations, focusing especially on those that extend the previous versions. Details of the calculations are embedded in the code and described in the code and the text.

The *pmf* and its partitioning into $\Delta\psi$ and ΔpH .

The theory and equations used to describe *pmf* components are essentially as described in earlier work by Cruz et al., (2001) and Zaks et al. (2012), with two updates. First, the new code allows for addition of antiporters or symporters, as described in the code for KEA3, which is proposed to act as a K⁺/H⁺ antiporter in the thylakoid membrane (28, 29):

#the KEA reaction looks like this:



Where H_{lumen}^+ , H_{stroma}^+ , K_{lumen}^+ , and K_{stroma}^+ represent protons in the lumen and stroma and K⁺ ions in the lumen and stroma, respectively. The reaction is electroneutral, so the forward reaction will depend on $\Delta[H^+]$ and $\Delta[K^+]$ as:

$$v_{KEA} = v_{KEA} ([H_{lumen}^+] \cdot [K_{stroma}^+] - [H_{stroma}^+] [K_{lumen}^+]) \quad (\text{Eq. 2})$$

$$v_{KEA} = k_{KEA} * (H_{lumen} * K_{stroma} - H_{stroma} * K_{lumen}) \quad (\text{Python})$$

where H_{lumen}^+ (H_{lumen}), H_{stroma}^+ (H_{stroma}), K_{lumen}^+ (K_{lumen}), K_{stroma}^+ (K_{stroma}) are the concentrations of free H⁺ and K⁺ ions in the lumen and stroma, respectively.

#Next, the following is used to calculate K⁺ flux, which depends on the permeability of electrogenic K⁺ channels and the KEA reaction. The permeability of K⁺ through the K⁺ channel is perm_K. The K⁺ flux through the electrogenic channel depends on both the K⁺ concentration gradient and the electric field, i.e. $\Delta\tilde{\mu}_{K^+}$,

$$\Delta\tilde{\mu}_{K^+} = .06(\log_{10} \left(\frac{[K^+]_{stroma}}{[K^+]_{lumen}} \right) - \Delta\psi \text{ (Eq. 3)}$$

$$K_deltaG = (.06 * np.log10(Kstroma/Klumen) - Dy) \text{ (Python)}$$

where $K_deltaG = \Delta\tilde{\mu}_{K^+}$ and $Dy = \Delta\psi$, the transthylakoid electric field (stroma-lumen) in V.

The instantaneous net change in lumen $[K^+]$ per unit time is given by:

$$\frac{d[K^+]}{dt} = v_{KEA} + P_{K^+} \Delta\tilde{\mu}_{K^+} ([K^+]_{lumen} + [K^+]_{stroma}) / 2 \text{ (Eq. 3)}$$

$$net_Klumen = perm_K * K_deltaG * (Klumen + Kstroma) / 2 + v_KEA \text{ (Python)}$$

where $net_Klumen = \frac{d[K^+]}{dt}$. In this simplified form, we assume that the flux through the K^+ channel is proportional to the driving force and the average concentration of K^+ in the stroma and lumen.

PSII recombination reactions and singlet O_2 production

Earlier work (e.g. (30) (31, 32)) shows that both $\Delta\psi$ and ΔpH should increase PSII recombination rates, and thus should increase 1O_2 production. We derived an equation for estimating recombination rate in PSII is described in Davis et al (2016) considering the effects of ΔpH and $\Delta\psi$ on energetics of electron sharing between redox intermediates:

:

$$v_{recomb} = [S_2 Q_A^-] * k_{recomb} 10^{(f_{\Delta\psi} \frac{-\Delta\psi}{0.06} + f_{pH} \cdot \Delta pH)} \text{ (eq. 4)}$$

$$v_recomb = k_recomb * QAm * (10^{*(fraction_Dy_effect * Dy /.06 + fraction_pH_effect * (7.0 - pHlumen))}) \text{ (Python)}$$

where v_{recomb} is the rate of recombination, $[S_2 Q_A^-]$ is the concentration of PSII centers with reduced QA and the oxygen evolving complex in the S_2 state, k_{recomb} the intrinsic rate of recombination from $S_2 Q_A^-$ in the absence of $\Delta\psi$ and ΔpH , ΔE_{stab} the stabilization free energy of the charge separated state, expressed in eV (Davis et al. 2016), $f_{\Delta\psi}$ (fraction_Dy_effect) and $f_{\Delta pH}$ (fraction_pH_effect) represents the fraction of quasi-stable S-states (that are able to recombine) and are sensitive to $\Delta\psi$ and ΔpH respectively (see text for more detail).

Normalizations of parameters

One (trivial) difference with our earlier model Cruz et al., (2001) is that content and concentration parameters are normalized to PSII content rather than thylakoid surface area. This will make it easier to account for lumen volume changes. We use the general parameters from the literature, as reviewed in Cruz et al., (2001), including the following. From Cruz et al., 2001 "...we estimated that there were approximately 2×10^{-13} mol of PSII cm^{-2} thylakoid membrane, or 6×10^{10} PSII complexes cm^{-2} . If all PSII centers were hit, on average there would be $6 \times 10^{10} \text{ cm}^{-2}$ protons delivered into the lumen.

2×10^{-13} mol of PSII cm^{-2} thylakoid membrane

6.02×10^{23} molecules per mole $\times 10^{-13}$ moles of PSII cm^{-2} thylakoid membrane

1.2×10^{11} PSII centers per cm^{-2} thylakoid membrane

1.2×10^{11} protons cm^{-2} , into 0.8×10^{-9} L cm^{-2} i.e. 2.3×10^{-6} moles/L are moved, equivalent to a change in the concentration of protons (both bound and unbound) of 2.3×10^{-5} moles or about 12 μM .

With 0.8×10^{-9} L lumen volume cm^{-2} thylakoid membrane, yield 1.2×10^{11} PSII centers per cm^{-2} thylakoid membrane, or 6.7×10^{-21} L per PSII center. Therefore, one turnover of PSII should introduce about 1.7×10^{-24} moles H^+ / 6.7×10^{-21} L equivalent to a change in concentration of about 2.5×10^{-4} M.

Given the large lumen buffering capacity, $\beta=0.03$ M/pH unit (), the vast majority of these protons become buffered, and a single turnover flash should yield a ΔpH change of only about 0.008 units. On the other hand, the capacitance of the thylakoid membrane is expected to be small, about $0.6 \mu\text{F}/\text{cm}^2$ (see text) so that moving one charge per PSII center should produce a substantial $\Delta\psi$,

Hitting all PSII centers with a single turnover flash should move 1.2×10^{11} charges cm^{-2} or 1.2×10^{11} charges / 6.242×10^{18} charges coulomb $^{-1}$ = 1.9×10^{-8} C, and with $1.9 \times 10^{-8} \text{ C} / 0.6 \times 10^{-6} \text{ C/V}$, and thus:

$$\Delta\psi(\text{flash}) = 0.033 \text{ V}$$

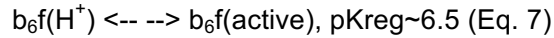
We use this value to indicate the effective $\Delta\psi$ for a transthylakoid movement of one charge per PSII equivalent.

The reactions of the cytochrome b_6f complex

The overall reaction for the cytochrome b_6f complex is taken to be:



where PQ and PQH₂ are the oxidized and reduced forms of plastoquinone, PC(ox) and PC(red) are the oxidized and reduced forms of plastocyanin, and pmf is the proton motive force. There are several factors to consider. First, there is a kinetic effect of lumen pH on the binding of PQH₂ to the Rieske Fe₂S₂ protein (21), with a pK_a near 6-6.5 (see (7) and references within), so that:



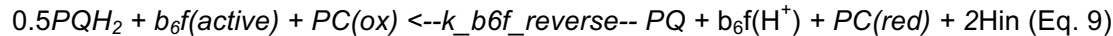
Where b₆f(active) is the deprotonated, active and b₆f(H⁺) is inactive forms of the complex. This is a kinetic constraint, likely related to the deprotonation of a His residue on the Rieske FeS protein, see Wang et al. (21), for a detailed description of the experimental bases of this interpretation in the cytochrome bc1 complexes. The term, pKreg, describes the pH-dependence of activation of the cytochrome b₆f complex. The empirically measured value is between 6.0 and 6.5 (7).

Next, we need to consider the redox states of PQH₂, PC as well as the Δψ and ΔpH components of pmf. Because the Q-cycle releases 2 H⁺ into the lumen for each electron passed from PQH₂ to PC, there should be a thermodynamic constraint to the forward reaction:



This is somewhat simplified in that the intermediate reactions involving electron transfer through the low potential cytochrome b chain are ignored and it is assumed that the electron from the semiquinone generated in the Q_o site of the complex is immediately transferred to PQ, so that while one PQ is produced during the Q_o site reaction, it is partially reduced with the net effect of oxidation of a 0.5 PQH₂.

The forward rate constant is k_{b6f}, but the reaction is reversible, so that



k_{b6f_reverse} is a function of pmf because the Q-cycle in the forward direction works against both ΔpH and Δψ. Note that this thermodynamic effect is in addition to the kinetic effect on the deprotonation of the Rieske protein. We simulate this as follows:

$$K_{eq,b6f} = E_m \left(\frac{PC_{ox}}{PC_{red}} \right) - E_m \left(\frac{PQ}{PQH_2} \right) - n \cdot pmf \text{ (Eq. 10)}$$

$$K_{eq_b6f} = E_m(PC(ox)/PC(red)) - E_m(PQ/PQH_2) - n^*pmf \text{ (Python)}$$

where K_{eq,b6f} is the equilibrium constant for the forward reaction, and E_m(Pc(ox)/PC(red)) = 0.370 V and E_m(PQ/PQH₂) = 0.11 V at pH=7, are the effective redox midpoint potentials for the PC and PQ couples at pH=7, but are pH-dependent so that:

$$E_m(\text{PQ}/\text{PQH}_2) = 0.11 \text{ V} - (7 - \text{pH}_{\text{lumen}}) \cdot 0.06 \text{ (Eq. 12)}$$

. In other words, the overall equilibrium constant is determined by the redox potentials of the donor and acceptor together and the pmf. We use unity as the scaling factor for the *pmf* contributions because one proton translocated to the lumen per e⁻ transferred (together with one e⁻ charge moved from the p- to the n-side) equilibrium.

$$k_{b6f,reverse} = \frac{k_{b6f,forward}}{K_{eq,b6f}} \text{ (Eq.13)}$$

$$k_b6f_reverse = k_b6f / K_{eq_b6f} \text{ (Python)}$$

In principle, we could simulate the effects of changing PQH₂ and PC redox states in two ways, either using the simulated concentrations of PQH₂ and PC together with the standard E'⁰ (E_m) values, or accounting for the concentrations in the E_m values. We chose the former because it better fits the form of the ODE equations and is a bit simpler to calculate. Thus,

$$v_{b6f} = [\text{PQH}_2][\text{PC}_{ox}]k_{b6f,forward} - [\text{PQ}][\text{PC}_{red}]k_{b6f,reverse} \text{ (eq. 14)}$$

$$v_b6f = [\text{PQH}_2][\text{PC}_{ox}]k_b6f - [\text{PQ}][\text{PC}_{red}]k_b6f_reverse \text{ (Python)}$$

The midpoint potential of PC is pH-independent under our conditions, but E'⁰(PQ/PQH₂) = 0.11 V at pH=7, but pH-dependent (see Eq. 12) so that:

$$K_{eq,b6f} = E_m\left(\frac{\text{PC}_{ox}}{\text{PC}_{red}}\right) - E_m\left(\frac{\text{PQ}}{\text{PQH}_2}\right) - n \cdot \text{pmf} = 0.370 - 0.11 + .06 \cdot (\text{pH}_{\text{lumen}} - 7.0) - n \cdot \text{pmf} \text{ (Eq. 15)}$$

$$K_{eq_b6f} = E'_0(\text{Pc}_{ox}/\text{PC}_{red}) - E'_0(\text{PQ}/\text{PQH}_2) - \text{pmf} = 0.370 - 0.11 + .06 \cdot (\text{pH}_{\text{lumen}} - 7.0) - \text{pmf} \text{ (Python)}$$

So, the full set of equations in Python is:

$$\text{Em7_PC} = 0.37 \quad \text{Em_PC} = \text{Em7_PC} \quad \text{Em7_PQH}_2 = 0.11 \quad \text{Em_PQH}_2 = \text{Em7_PQH}_2 + 0.06 \cdot (\text{pH}_{\text{lumen}} - 7.0) \text{ \#(Eq. 16)}$$

$$K_{eq_b6f} = 10^{((\text{Em_PC} - \text{Em_PQH}_2) - \text{pmf})/.06} \text{ \#(Eq. 17)}$$

$$k_b6f_reverse = k_b6f / K_{eq} \text{ \# (Eq. 18)}$$

$$v_b6f = \text{PQH}_2 \text{PC}_{ox} k_b6f - \text{PQPC}_{red} k_b6f_reverse \text{ \# (Eq. 19)}$$

Calculating Phi2

The following is a derivation for determining Phi2 from NPQ and QA redox state. The equations and derivations are based on those presented in Kramer et al. (33).

Recall that NPQ is the ratio of:

$$NPQ = \frac{k_{NPQ}}{k_f + k_d} \text{ (Eq. 20)}$$

where k_{NPQ} , k_f and k_d are the intrinsic rate constants for NPQ, fluorescence and non-radiative decay of excitons in the photosynthetic antenna. Also, maximal PSII quantum yield is:

$$\phi_{II,max} = \frac{k_{pc}}{k_d + k_f + k_{pc}} \sim 0.8 \text{ (Eq. 21)}$$

$$\frac{1}{\phi_{II,max}} = \frac{k_d + k_f + k_{pc}}{k_{pc}} = 1 + \frac{k_d + k_f}{k_{pc}} \text{ (Eq. 22)}$$

$$\frac{k_{pc}}{k_d + k_f} = \frac{1}{\frac{1}{\phi_{II,max}} - 1} \sim 4.88 \text{ (Eq. 23)}$$

where k_{pc} is the maximal rate constant for PSII photochemistry.

The realized ϕ_{II} at any time is given by:

$$\phi_{II} = \frac{[QA]k_{pc}}{k_d + k_f + k_{NPQ} + [QA]k_{pc}} \text{ (Eq. 24)}$$

where $[QA]$ is the fraction of open PSII centers with oxidized Q_A .

$$\frac{1}{\phi_{II}} = \frac{k_d + k_f + k_{NPQ} + [QA]k_{pc}}{[QA]k_{pc}} = 1 + \frac{k_d + k_f + k_{NPQ}}{[QA]k_{pc}} = 1 + \frac{k_d + k_f}{[QA]k_{pc}} + \frac{k_{NPQ}}{[QA]k_{pc}} = 1 + \frac{k_d + k_f}{[QA]k_{pc}} + \frac{NPQ(k_f + k_d)}{[QA]k_{pc}} \text{ (Eq. 25)}$$

$$[Q_A] \left(\frac{1}{\phi_{II}} - 1 \right) = \frac{k_d + k_f}{k_{pc}} + \frac{NPQ(k_f + k_d)}{k_{pc}} = \frac{k_d + k_f}{k_{pc}} (1 + NPQ) = \frac{(1 + NPQ)}{4.88} \text{ (Eq. 26)}$$

$$\frac{1}{\phi_{II}} - 1 = \frac{(1 + NPQ)}{4.88[Q_A]} \text{ (Eq. 27)}$$

$$\frac{1}{\phi_{II}} = \frac{(1 + NPQ)}{4.88[Q_A]} + 1 \text{ (Eq. 28)}$$

$$\phi_{II} = \frac{1}{\frac{(1 + NPQ)}{4.88[Q_A]} + 1} \text{ (Eq. 29)}$$

In Python, this translates to:

```
def Calc_Phi2(QA, NPQ):
    Phi2=1/(1+(1+NPQ)/(4.88*QA))
    return Phi2
```

References to Notes

1. Vredenberg WJ (1976) Electrical interactions and gradients between chloroplast compartments and cytoplasm. *The Intact Chloroplast*, ed Barber J (Elsevier/North Holland Biomedical Press, The Netherlands), pp 53-87.
2. Junge W, Ausländer W, McGeer AJ, & Runge T (1979) The buffering capacity of the internal phase of thylakoids and the magnitude of the pH changes inside under flashing light. *Biochim. Biophys. Acta* 546:121-141.
3. Hope AB (2000) Electron transfers amongst cytochrome f, plastocyanin and photosystem I: kinetics and mechanisms. *Biochim. Biophys. Acta* 1456:5-26.
4. Jahns P, Graf M, Munekage Y, & Shikanai T (2002) Single point mutation in the Rieske iron-sulfur subunit of cytochrome b(6)/f leads to an altered pH dependence of plastoquinol oxidation in Arabidopsis. *FEBS Lett* 519(1-3):99-102.

5. Kirchhoff H, Horstmann S, & Weis E (2000) Control of the photosynthetic electron transport by PQ diffusion microdomains in thylakoids of higher plants. *Biochim Biophys Acta* 1459(1):148-168.
6. Takizawa K, Cruz JA, & Kramer DM (2008) Depletion of stromal inorganic phosphate induces high 'energy-dependent' antenna exciton quenching (q_E) by decreasing proton conductivity at CF₀-CF₁ ATP synthase. *Plant, cell & environment* 31 235-243.
7. Takizawa K, Kanazawa A, Cruz JA, & Kramer DM (2007) In vivo thylakoid proton motive force. Quantitative non-invasive probes show the relative lumen pH-induced regulatory responses of antenna and electron transfer. *Biochim Biophys Acta* 1767 1233–1244.
8. Takizawa K, Cruz JA, & Kramer DM (2005) *In vivo* estimations of lumen acidification and q_E response using calibrated electrochromic shift assays. *Photosynthesis: Fundamental Aspects to Global Perspectives*, eds van der Est A & Bruce D (ACG Publishing), pp 573-575.
9. Avenson TJ, *et al.* (2005) Integrating the proton circuit into photosynthesis: Progress and challenges. *Plant, cell & environment* 28:97-109.
10. Schottler MA, Toth SZ, Boulouis A, & Kahlau S (2015) Photosynthetic complex stoichiometry dynamics in higher plants: biogenesis, function, and turnover of ATP synthase and the cytochrome b6f complex. *J Exp Bot* 66(9):2373-2400.
11. Vredenberg WJ & Bulychev AA (1976) Changes in the electrical potential across the thylakoid membranes of illuminated intact chloroplasts in the presence of membrane-modifying agents. *Plant Sci Lett* 7:101-107.
12. Cruz JA, Sacksteder CA, Kanazawa A, & Kramer DM (2001) Contribution of electric field ($\Delta\psi$) to steady-state transthylakoid proton motive force *in vitro* and *in vivo*. Control of *pmf* parsing into $\Delta\psi$ and ΔpH by counterion fluxes. *Biochemistry* 40:1226-1237.
13. Seelert H, Dencher NA, & Muller DJ (2003) Fourteen protomers compose the oligomer III of the proton-rotor in spinach chloroplast ATP synthase. *J Mol Biol* 333(2):337-344.
14. Ueno H, Suzuki T, Kinoshita K, Jr., & Yoshida M (2005) ATP-driven stepwise rotation of FoF1-ATP synthase. *Proc Natl Acad Sci U S A* 102(5):1333-1338.
15. Giersch C, *et al.* (1980) Energy charge, phosphorylation potential and proton motive force in [spinach] chloroplasts. *Biochim Biophys Acta* 590:59-73.
16. Wu W & Berkowitz GA (1992) Stromal pH and photosynthesis are affected by electroneutral K⁺ and H⁺ exchange through chloroplast envelope ion channels. *Plant Physiol* 98:666-672.
17. Heldt HW, Werdan K, Milovancev M, & Geller G (1973) Alkalization of the chloroplast stroma caused by light-dependent proton flux into the thylakoid space. *Biochim. Biophys. Acta* 314:224-241.

18. Pfündel EE & Dilley RA (1993) The pH dependence of violaxanthin deepoxidation in isolated pea chloroplasts. *Plant Physiol* 101:65-71.
19. Yamamoto HY (1979) Biochemistry of the violaxanthin cycle in higher plants. *Pure Appl. Chem.* 51:639-648.
20. Siefermann D & Yamamoto HY (1975) Properties of NADPH and oxygen-dependent zeaxanthin epoxidation in isolated chloroplasts. *Biochem.* 171:70-77.
21. Crofts AR & Wang Z (1989) How rapid are the internal reactions of the ubiquinol: cytochrome c_2 oxidoreductase? *Photosynth. Res.* 22:69-87.
22. Rich PR (1985) Mechanisms of quinol oxidation in photosynthesis. *Photosynth Res* 6(4):335-348.
23. Cooley JW, Nitschke W, & Kramer DM (2008) The cytochrome bc_1 and related bc complexes, the Rieske/cytochrome b complex as the functional core of a central electron/proton transfer complex. *The Purple Photosynthetic Bacteria*, eds Hunter CN, Daldal F, Thurnauer MC, & Beatty JT (Springer, Dordrecht, The Netherlands), pp 451-473.
24. Sykes AG (1991) Plastocyanin and blue copper proteins. *Struct. Bond.* 75:175-224.
25. Schottler MA, Kirchhoff H, & Weis E (2004) The role of plastocyanin in the adjustment of the photosynthetic electron transport to the carbon metabolism in tobacco. *Plant Physiol* 136(4):4265-4274.
26. Kirchhoff H, Schottler MA, Maurer J, & Weis E (2004) Plastocyanin redox kinetics in spinach chloroplasts: evidence for disequilibrium in the high potential chain. *Biochim Biophys Acta* 1659(1):63-72.
27. Crofts AR & Wraight CA (1983) The electrochemical domain of photosynthesis. *Biochim. Biophys. Acta* 726:149-185.
28. Kunz HH, *et al.* (2014) Plastidial transporters KEA1, -2, and -3 are essential for chloroplast osmoregulation, integrity, and pH regulation in Arabidopsis. *Proc Natl Acad Sci U S A* 111(20):7480-7485.
29. Armbruster U, *et al.* (2014) Ion antiport accelerates photosynthetic acclimation in fluctuating light environments. *Nature communications* 5:5439.
30. Jursinic P, Govindjee, & Wraight CA (1978) Membrane Potential and Microsecond to Millisecond Delayed Light Emission After a Single Excitation Flash in Isolated Chloroplasts. *Photochem. Photobiol.* 27:61-71.
31. Wagner H, Gilbert M, Goss R, & Wilhelm C (2006) Light emission originating from photosystem II radical pair recombination is sensitive to zeaxanthin related non-photochemical quenching (NPQ). *J Photochem Photobiol B* 83(3):172-179.
32. Crofts AR & Wraight CA (1971) Energy conservation in the photochemical reactions of photosynthesis and its relation to delayed fluorescence. *FEBS Lett* 15(2):89-100.
33. Kramer DM, Johnson G, Kiirats O, & Edwards GE (2004) New fluorescence parameters for the determination of Q_A redox state and excitation energy fluxes. *Photosynthesis research* 79:209-218.